Journal of Materials Chemistry B

Accepted Manuscript

ROYAL SOCIETY OF CHEMISTRY

www.rsc.org/materialsB

Tunable thermo-responsive P(NIPAAm-*co*-DMAAm)-*b*-PLLA-*b*-P(NIPAAm-*co*-DMAAm) triblock copolymer micelles as drug carrier

Yanfei Hu,[a] Vincent Darcos,[a] Sophie Monge,[b] Suming Li[a]*, Yang Zhou,[c] Feng Su[c]

[a] Institut des Biomolécules Max Mousseron, UMR CNRS 5247 – Equipe Biopolymères Artificiels, Université Montpellier I, 15 Avenue Charles Flahault, BP 14491, 34093 Montpellier, France.

[b] Institut Charles Gerhardt, UMR 5253 CNRS-UM2-ENSCM-UM1 - Equipe Ingénierie et Architectures Macromoléculaires, Université Montpellier II, cc1702, Place Eugène Bataillon, 34095 Montpellier, France.

[c] College of Chemical Engineering, Qingdao University of Science and Technology, 266042 Qingdao, China

Correspondence to: Suming Li (E-mail: lisuming@univ-montp1.fr)

Abstract

Thermo-responsive triblock copolymers were synthesized by atom transfer radical polymerization of *N*-isopropyl acrylamide (NIPAAm) and *N,N*-dimethyl acrylamide (DMAAm) using α,ω-bromopropionyl poly(L-lactide) as macro-initiator and a CuCl/tris(2-dimethylaminoethyl) amine (Me_6TREN) complex as catalyst. The polymerization was realized at 25 °C in a DMF/water mixture. DMAAm was incorporated in the copolymer as a hydrophilic comonomer in order to tune the lower critical solution temperature (LCST). The LCST linearly increases from 32.2 to 39.1 °C with increasing the DMAAm content from 0 to 24 %. The phase transition of polymeric micelles at the LCST occurs in a narrow temperature interval below 0.5 °C. Reversible size changes are observed when the temperature increases from 25 to 45 °C and then decreases down to 25 °C. Nano-size micelles (37 to 54 nm) with narrow distribution were obtained by self-assembly of amphiphilic copolymers in aqueous medium. The critical micelle concentration (CMC) ranges from 0.010 to 0.015 mg mL^{-1}. *In vitro* drug release studies show a much faster release at temperatures above the LCST. MTT assay was conducted to evaluate the cytotoxicity of copolymers. Therefore, the nano-scale size, low CMC, rapid phase transition, LCST slightly above the body temperature and thermo-responsive drug release indicate that these copolymers could be potential candidates for applications in targeted delivery of drugs.

Keywords: Thermo-responsive copolymer; Poly(*N*-isopropyl acrylamide); Poly(L-lactide)

Introduction

Recently, smart micelles derived from stimuli-responsive polymers have drawn great attention as drug delivery systems (DDS).[1-3] Among them, thermo-sensitive copolymers based on poly(*N*-isopropyl acrylamide) (PNIPAAm) have been widely investigated, notably to build polymeric micelles for controlled delivery of anticancer drugs or DNA.[4-10] PNIPAAm could be considered as the "gold standard" thermo-responsive polymer with a lower critical solution temperature (LCST) around 32 ^{o}C, which is induced by a reversible hydration-dehydration transition.[11,12] Variation of pH, concentration, chemical structure or biological environment only slightly affects the LCST. However, these copolymers are not degradable, which limits their potential applications as drug carrier.

As a biodegradable polymer, polylactide (PLA) has been extensively investigated for biomedical and pharmaceutical applications such as controlled drug release systems, medical implants and scaffolds in tissue engineering.[13-16] Block copolymers based on PNIPAAm and PLA combine both the thermo-sensitivity of PNIPAAm and the degradability of PLA.[17-22] Increasing the temperature above the LCST results in collapse of micelles and burst-like release of encapsulated drug.[21] Thus temporal drug delivery could be achieved by using thermo-sensitive and degradable polymeric micelles based on PLA and PNIPAAm.

The PNIPAAm moiety is supposed to be soluble in the blood stream, and becomes insoluble after accumulation in a locally heated tumor tissue. This property could be exploited for targeted delivery of drugs.[23-26] Therefore, polymeric micelles should be designed so as to exhibit a LCST slightly above the body temperature. Introducing hydrophilic acrylamide comonomers such as dimethyl acrylamide (DMAAm) in PNIPAAm chains has been used to increase the LCST of the resulting copolymers. Most of the P(NIPAAm-*co*-DMAAm)-*b*-PLA diblock copolymers described in the

literature were synthesized by combination of free radical polymerization and ring-opening polymerization (ROP).[27-33] The resulting copolymers exhibit poorly defined compositions and large molecular weight distributions (dispersity $Đ$ >2), which led to a broad phase transition at the LCST. Later on, Akimoto et al. synthesized well-defined P(NIPAAm-*co*-DMAAm)-*b*-PLA diblock copolymers by combination of reversible addition-fragmentation chain transfer polymerization (RAFT) and ROP.[34-37] The terminal dithiobenzoate (DTBz) groups were reduced to thiol groups and reacted with maleimide (Mal). In aqueous media, the resulting copolymers formed surface-functionalized thermo-responsive micelles, hydrophobic DTBz-surface micelles demonstrating a significant lower LCST (30.7 °C) than Mal-surface micelles (40.0 °C). The LCST of micelle mixtures can be varied by changing the ratio of DTBz/Mal end-functional diblock copolymers.[34] The authors also studied thermally controlled intracellular uptake of copolymer micelles.[35-36] Li et al. reported similar maleimide end-functional P(NIPAAm-*co*-DMAAm)-*b*-PLA and P(NIPAAm-*co*-DMAAm)-*b*-PCL copolymers with LCST of 39 °C and 40.5 °C, respectively.[37] Both the adriamycin release and the intracellular uptake was enhanced at 40°C as compared to 37 °C. However, precise tuning of the LCST could not be achieved by modification of endgroups or mixing two copolymers with different endgroups.

In a previous paper, we reported, for the first time, the synthesis of thermo-sensitive PNIPAAm-*b*-PLA-*b*-PNIPAAm triblock copolymers by atom transfer radical polymerization (ATRP) using α,ω-bromopropionyl poly(L-lactide) (PLLA) as macroinitiator.[38] Excellent control over the molecular weights was achieved under mild conditions. The kinetics of polymerization and the self-assembly behavior of the resulting copolymers were investigated. However, the LCST of the copolymers ranges from 32.1 to 32.8 °C, *i.e*. much lower than the body temperature.

In this work, thermo-responsive and biodegradable P(NIPAAm-*co*-DMAAm)-*b*-PLLA-*b*-P(NIPAAm-*co*-DMAAm) triblock copolymers were prepared via combination of ROP and ATRP. DMAAm comonomer was introduced in order to tune the LCST slight above body temperature for targeted drug delivery in tumor tissue. The resulting copolymers were fully characterized by ^{1}H NMR, SEC and DOSY NMR. The physico-chemical properties of copolymer micelles were investigated in aqueous media. MTT assays were carried out to evaluate the cytotoxity of copolymers. The drug release behavior of micelles containing an antimicrobial agent, Amphotericin B, was investigated below and above the LCST.

Experimental Methods

Materials

L-lactide was purchased from Purac Biochem (Goerinchem, The Netherlands). Stannous 2-ethyl hexanoate ($Sn(Oct)_2$), 1,4-benzene dimethanol, 2-bromopropionyl bromide, tris(2-dimethyl aminoethyl) amine (Me_6TREN), copper (I) chloride (CuCl), N,N-dimethyl formamide (DMF) and Amphotericin B were obtained from Sigma-Aldrich (St-Quentin Fallavier, France), and were used without further purification. Dichloromethane and toluene from Sigma-Aldrich were dried over calcium hydride for 24 h at room temperature and distilled under reduced pressure. NIPAAm and DMAAm were obtained from Sigma-Aldrich and purified through a basic aluminum oxide column. Triethylamine (Sigma-Aldrich) was dried over potassium hydroxyde for 24 h at room temperature and distilled. Ultrapure water with a conductivity of 18MΩ was produced using a Millipore Milli-Q water system.

α,ω-bromopropionyl PLLA (Br-PLLA-Br) was prepared as previously reported.[38]

Typical synthesis of P(NIPAAm-*co*-DMAAm)-*b*-PLLA-*b*-P(NIPAAm-*co*-DMAAm) *(Run T4, Table 2)*

Triblock copolymers were prepared using standard Schlenk technique. Typically, 100 mg Br-PLLA-Br (30.4×10^{-3} mmol, $M_{n,NMR}$= 3300 g mol^{-1}), 572 mg NIPAAm (5.06 mmol), 1.07 mL DMAAm (1.03 mmol) and 6.0 mg CuCl (60.8×10^{-3} mmol) were dissolved in 3 mL DMF in a Schlenk tube. 0.6 mL H_2O was then added. After five freeze-pump-thaw cycles, 16µL Me_6TREN (60.8×10^{-3} mmol) was added under argon atmosphere. The mixture was stirred at 25 ^oC for 1 h. The reaction was stopped by precipitation in diethyl ether, and the crude product was dissolved in 10 mL chloroform. The diluted polymer solution was allowed to pass through a basic aluminum oxide column to remove the catalyst complex, concentrated under reduced pressure, and precipitated again in diethyl ether. The final product was dried under vacuum at room temperature for 24 h.

^{1}H NMR (300 MHz, $CDCl_3$) (Fig. 1) δ (ppm)=7.28 (s, $4H_{Ar}$), 5.20 (m $1H_a$), 4.00 (m, $1H_e$), 2.90 (d, $3H_g$), 2.09 (t, $1H_{d+d'}$), 1.78 (d, $2H_{c+c'}$), 1.58(d, $3H_b$), 1.13(d, $3H_f$)

$M_{n,NMR}$=20000 g mol^{-1}, $M_{n,SEC}$=24000 g mol^{-1}, $Đ$=1.13.

Drug release studies

Amphotericin B (AmpB, 2.5 or 5 mg) and copolymer T4 (20 mg) were dissolved in 2 mL DMSO. The solution was then dropped into 40 mL ultrapure water. After 30 min stirring, the solution was introduced into a dialysis tube (MWCO 3500) and dialyzed against water for 48 hours. The dialyzed solution was filtered with 0.45 µm syringe filter to remove excess drug and then lyophilized. Blank copolymer micelles were prepared using the same procedure without AmpB.

The drug content and loading efficiency were determined by UV spectroscopy. 5 mg AmpB-encapsulated polymeric micelles were dissolved in DMSO. UV measurements were realized at 388

nm. The concentration of AmpB was determined using a calibration curve obtained with a series of standard AmpB solutions in DMSO. The drug loading content and loading efficiency were calculated using the following equations:

$$\text{Drug content } (wt\ \%) = 100 \times \text{Weight of drug in micelles} / \text{Weight of drug loaded micelles} \quad (1)$$

$$\text{Loading efficiency } (wt\ \%) = 100 \times \text{Weight of drug in micelles} / \text{Weight of feeding drug} \quad (2)$$

Drug release studies were carried out at two different temperatures. Briefly, 5 mg lyophilized polymeric micelle was reconstituted in 5 mL ultrapure water and then introduced into a dialysis tube (MWCO: 3500). The dialysis tube was placed in 20 mL ultrapure water in oven at 37 or 38 ^{o}C. At preset time intervals, the release medium was recovered for analysis and renewed with fresh ultrapure water. The drug concentration was determined by UV spectroscopy at 388 nm.

Cytotoxicity

The cytotoxicity of polymers was evaluated by MTT assay. After sterilization by UV for 5 h, the copolymer T4 was dissolved in Dulbecco's Modified Eagle's Meduim (DMEM, Hyclone products) at a concentration of 6 mg mL^{-1}. Then the solution was transferred to 96-well plates (Corning costar, USA), 100 μL per well. The wells were placed in an incubator (NU-4850, NuAire, USA) at 37 ^{o}C under humidified atmosphere containing 5 % CO_2 for 24 h. After incubation, the copolymer in the form of a hydrogel was used as cell culture substrate.

Mouse cardiac myocytes (MCM) and mouse embryonic fibroblasts (MEF) in logarithmic growth phase were harvested and diluted with DMEM medium (10 % calf serum, 100 μg mL^{-1} Penicillin, 100 μg mL^{-1} streptomycin) to a concentration of 1×10^{5} cells mL^{-1}. 100 μL cellular solution was added

in hydrogel containing wells which were then placed in the same incubator at 37 ^{o}C under humidified atmosphere containing 5 % CO_2. 100 μL fresh medium was used as the negative control, and 100 μL solution of phenol and water as the positive control. After 2, 3 and 4 days culture, 20 μL 3-(4,5-dimethylthiazol-2-yl)-2,5-diphenyltetrazolium bromide (MTT) at 5 mg mL^{-1} were added. The medium was removed after 6 h incubation, and 150 μL dimethylsulfoxide (DMSO) was added. After 15 min shaking, the optical density (OD) was measured by using a microplate reader (Elx800, BioTek, USA) at 490 nm.

The relative growth ratio (RGR) was calculated by using the following equation:

$$RGR\ (\%)=(OD_{test\ sample}/OD_{negative\ Control})\times 100 \qquad (3)$$

The cytotoxicity is generally noted in 0-5 levels according to the RGR value as shown in Table 1.

Table 1. Relationship between the RGR value and cytotoxicity level

RGR (%)	≥100	75-99	50-74	25-49	1-24	0
Level	0	1	2	3	4	5

The cellular morphology was observed using an Olympus CKX41 inverted microscope. After 3 days seeding, the test medium was replaced with 150 μL neutral red staining solution (NR) for 10 min at room temperature. The plates were rinsed 3 times with warm phosphate-buffered saline (PBS), and the morphology of cells adhered to the hydrogel surface was immediately observed under microscope.

Characterization

^{1}H NMR spectra were recorded on a Bruker spectrometer (AMX300) operating at 300 MHz. Chemical shift was referenced to the peak of residual non-deuterated solvents.

DOSY 2D NMR measurements were performed at 300 K on a Bruker Avance AQS600 NMR

spectrometer operating at 600 MHz and equipped with a Bruker multinuclear z-gradient inverse probe head capable of producing gradients in the z direction with strength of 55 G cm^{-1}. The DOSY spectra were acquired with the ledbpgp2s pulse program from Bruker topspin software. All spectra were recorded with 32 K time domain data points in t_2 dimension and 32 t_1 increments. The gradient strength was logarithmically incremented in 32 steps from 2 % up to 95 % of the maximum gradient strength. All measurements were performed with a compromise diffusion delay Δ of 200 ms in order to keep the relaxation contribution to the signal attenuation constant for all samples. The gradient pulse length δ was 5 ms in order to ensure full signal attenuation. The diffusion dimension of the 2D DOSY spectra was processed by means of the Bruker topspin software (version 2.1). The DOSY maps were obtained with the Bruker topspin software (version 2.1).

SEC measurements were performed on a Varian 390-LC equipped with a refractive index detector and two ResiPore columns (300×7.5 mm) at 60 °C at a flow rate of 1 mL min^{-1}. The eluent was DMF containing 0.1 *wt* % LiBr. Calibration was established with PMMA standards.

The CMC of the copolymers was determined by fluorescence spectroscopy using pyrene as a hydrophobic fluorescent probe. Measurements were carried outon an RF 5302 Shimadzu spectrofluorometer (Japan) equipped with a Xenon light source (UXL-150S, Ushio, Japan). Briefly, an aliquot of pyrene solution (6×10^{-6} M in acetone, 1 mL) was added to different vials, and the solvent was evaporated. Then, 10 mL aqueous solutions at different concentrations were added to the vials. The final concentration of pyrene in each vial was 6×10^{-7} M. After equilibrating at room temperature overnight, the fluorescence excitation spectra of the solutions were recorded from 300 to 360 nm at an emission wavelength of 394 nm. The emission and excitation slit widths were 3 and 5 nm, respectively. The excitation fluorescence values I_{337} and I_{333}, respectively at 337 and 333 nm,

were used for subsequent calculations. The CMC was determined from the intersection of linear regression lines on the I_{337}/I_{333} ratio *versus* polymer concentration plots.

The lower critical solution temperature (LCST) was estimated from the changes in the transmittance through copolymer solutions at a concentration of 3.0 mg mL^{-1} as a function of temperature. The measurements were carried out at a wavelength of 500 nm with a Perkin Elmer Lambda 35 UV-Visible spectrometer equipped with a Peltier temperature programmer PTP-1+1. The temperature ramp was 0.1 °C min^{-1}.

DLS measurements were carried out with a Malvern Instrument Nano-ZS equipped with a He-Ne laser (λ = 632.8 nm). Polymer solutions at a concentration of 1.0 mg mL^{-1}were filtered through a 0.45 μm PTFE microfilter before measurements. The correlation function was analyzed via the general purpose method (NNLS) to obtain the distribution of diffusion coefficients (*D*) of the solutes. The apparent equivalent hydrodynamic radius (R_H) was determined from the cumulant method using the Stokes-Einstein equation:

$$R_H = \frac{k_B T}{6phG}\ q^2 = \frac{k_B T}{6phD_0} \qquad (4)$$

Where k_B is Boltzmann constant, T is the temperature, G is the relaxation frequency, q is the wave vector, h is the viscosity of the medium, and D_0 is the translational diffusion coefficient at finite dilution. Mean radius values were obtained from triplicate runs. Standard deviations were evaluated from hydrodynamic radius distribution.

TEM experiments were carried out on a JEOL 1200 EXII instrument operating at an acceleration voltage 120 kV. The samples were prepared by dropping a polymer solution at a concentration of 1.0 mg mL^{-1} onto a carbon coated copper grid, followed by air drying.

The residual copper content in the copolymers was quantified using a ThemoFinnigan Element XR

sector field ICP-MS (inductively coupled plasma-mass spectrometry) previously calibrated using copper solutions in water. Typically, ICPMS samples were prepared by dissolution of the copolymers in nitric acid. The solution was then heated to fully decompose the polymer until no precipitate was visible. After that, the samples were dissolved in 10 mL deionized water before analysis to determine the copper concentration. Each sample was analyzed four times.

Results and discussion

Synthesis of P(NIPAAm-*co*-DMAAm)-*b*-PLLA-*b*-P(NIPAAm-*co*-DMAAm)

Amphiphilic thermo-sensitive triblock copolymers, namely P(NIPAAm-*co*-DMAAm)-*b*-PLLA-*b*-P(NIPAAm-*co*-DMAAm), were synthesized by ATRP of NIPAAm and DMAAm using Br-PLLA-Br as macroinitiator (Scheme 1).

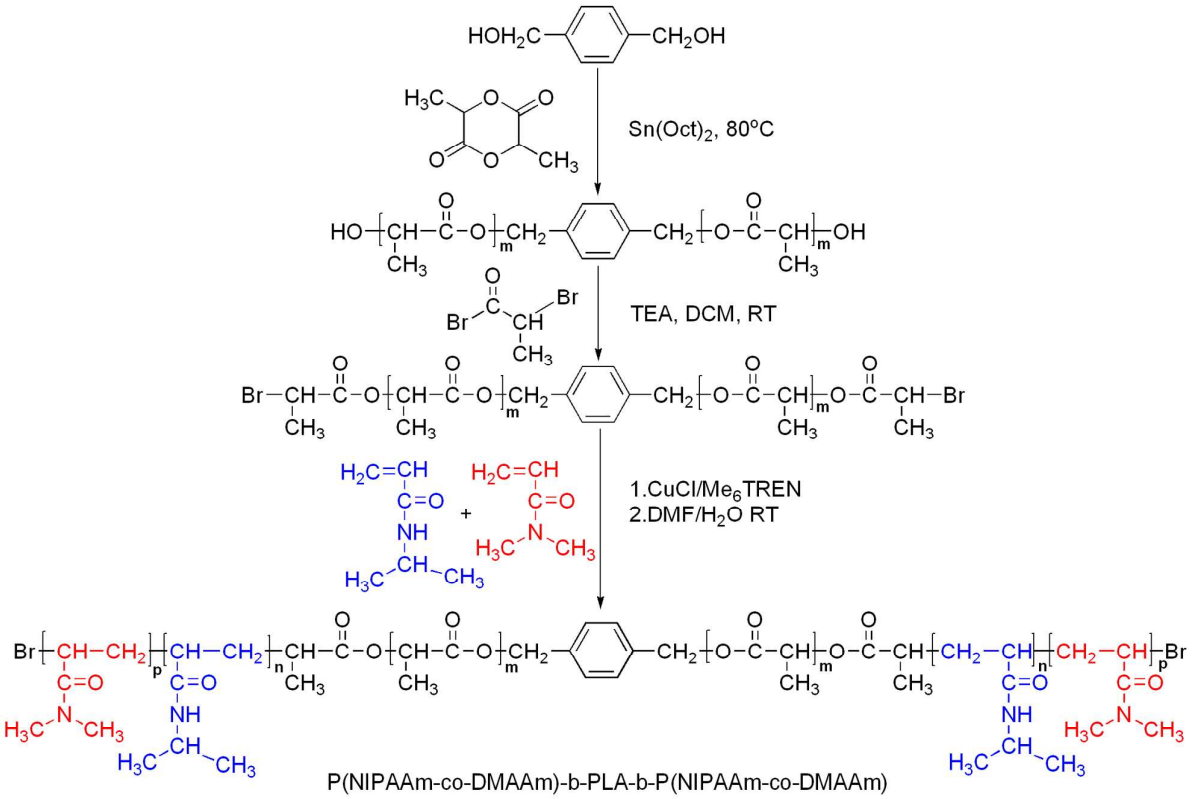

Scheme 1. Synthesis of P(NIPAAm-*co*-DMAAm)-*b*-PLLA-*b*-P(NIPAAm-*co*-DMAAm) triblock copolymers via combination of ROP and ATRP

In the first step, ring opening polymerization of L-lactide was carried out using 1,4-benzyl methanol as initiator to yield α,ω-hydroxy PLLA (HO-PLLA-OH). The targeted degree of polymerization (DP) of PLLA was 40 which corresponds to a theoretical Mn of 2900 g mol^{-1}. The M_n of HO-PLLA-OH determined by ^{1}H NMR was 3000 g mol^{-1}, i.e. very close to the targeted value. Moreover, the polymer exhibited a very low dispersity ($Đ$=1.03), in agreement with a good control of the reaction. In a second step, HO-PLLA-OH reacted with 2-bromopropionyl bromide in the presence of triethylamine, yielding α,ω-bromopropionyl PLLA (Br-PLLA-Br). The incorporation of bromopropionyl moiety was evidenced by ^{1}H NMR, and the anchoring proved to be quantitative. ^{1}H NMR and SEC analyses of Br-PLLA-Br ($M_{n,NMR}$= 3300 g mol^{-1}, $Đ$= 1.04) showed a slight increase of molecular weight and unchanged dispersity ($Đ$) compared to the starting HO-PLLA-OH, indicating that no chain cleavage occurred during the esterification reaction.

Then, α,ω-bromopropionyl PLLA was used as macroinitiator for ATRP copolymerization of NIPAAm and DMAAm at 25 °C in a DMF/water mixture using CuCl/Me_6TREN complex as catalytic system (Scheme1). A series of amphiphilic triblock copolymers were prepared by varying the NIPAAm to DMAAm ratio, but using a constant ratio of monomers to PLLA (200 equivalents) to yield copolymers with similar molecular weights (Table 2). This should allow to elucidate the influence of NIPAAm to DMAAm ratio on the LCST since the effect of hydrophobic to hydrophiphilic ratio is discarded. The conversion of NIPAAm was found to be around 70 %, while

the conversion of DMAAm is almost complete. This finding indicates that DMAAm exhibits higher reactivity than NIPAAm.[39, 40]

Table 2 Characteristics of P(NIPAAm-*co*-DMAAm)-*b*-PLLA$_{40}$-*b*-P(NIPAAm-*co*-DMAAm) triblock copolymers

Run	[PLA$_{40}$]/NIPAAm/ DMAAm[a]	DP$_{LA}$/DP$_{NIPAAm}$ /DP$_{DMAAm}$[b]	[NIPAAm] /[DMAAm][a]	$M_{n,NMR}$[b] g mol^{-1}	$M_{n,SEC}$[c] g mol^{-1}	$Đ$[c]
T1	1/200/0	40/172/0	100/0	22500	27000	1.10
T2	1/182.1/17.9	40/128/17	88.2/11.8	19500	25000	1.13
T3	1/172.6/27.4	40/116/25	82.8/17.2	19400	25700	1.15
T4	1/169.5/30.5	40/124/31	80.2/19.8	20000	24000	1.13
T5	1/164.6/35.4	40/112/34	76.9/23.1	19000	24000	1.18
T6	1/162.9/37.1	40/116/37	76.0/24.0	20000	23600	1.17

Conditions of ATRP: [M]$_0$=1.69 M, T=25 ^{o}C, [initiator]/[CuCl]/[Me$_6$TREN]=1/2/2, solvent mixture DMF/water=5/1.

[a] feed ratio. [b]calculated from ^{1}H NMR. [c] determined by SEC.

The chemical structure of triblock copolymers was characterized by ^{1}H and DOSY NMR spectroscopy. Fig. 1 shows the ^{1}H NMR spectrum of a copolymer in $CDCl_3$. The methyl (H_f, CH_3) and methine protons (H_e, CH) adjacent to the amine moiety of the NIPAAm units are observed at 1.1 and 4.0 ppm, respectively. The signal at 2.9 ppm is assigned to the methyl proton (H_g, CH_3) of DMAAm. The signals at 1.5 and 5.1 ppm are characteristic of the methyl (H_b) and methine protons (H_a, CH) of PLLA. The [LA]/[NIPAAm]/[DMAAm] ratio was calculated from the integrations of

the methine protons (-C*H*(CH_3)-) of lactyl units at 5.1 ppm, methine protons (-NHC*H*$(CH3)_2$-) of NIPAAm units at 4.0 ppm and methyl protons (-$(CH_3)_2$) of DMAAm at 2.9 ppm (equation 5). The DP of NIPAAm and DMAAm units, and the M_n of copolymers were then obtained using following equations:

$$[LA]/[NIPAAm]/[DMAAm] = I_a / I_e / (I_g/6) \quad (5)$$

$$DP_{NIPAAm} = DP_{LA} / ([LA]/[NIPAAm]) \quad (6)$$

$$DP_{DMAAm} = DP_{LA} / ([LA]/[DMAAm]) \quad (7)$$

$$M_{nNMR} = 72 \times DP_{LA} + 113 \times DP_{NIPAAm} + 98 \times DP_{DMAAm} \quad (8)$$

Where 72, 113 and 98 are the molar mass of LA, NIPAAm and DMAAm units, respectively.

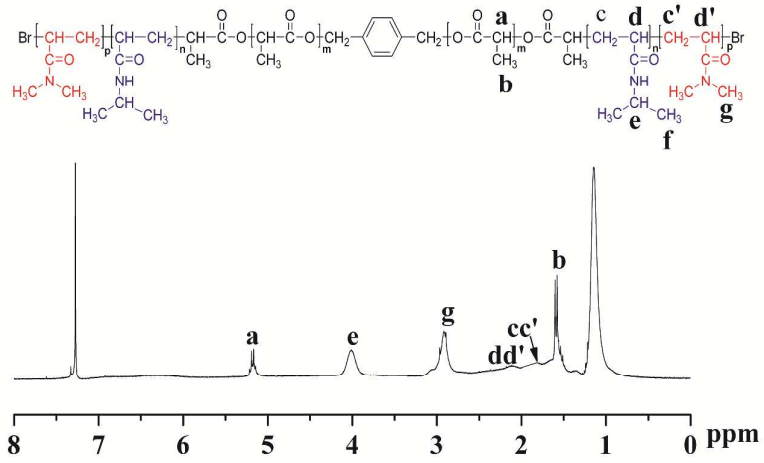

Fig. 1 ^{1}H NMR spectrum of P(NIPAAm-*co*-DMAAm)-*b*-PLLA-*b*-(PNIPAAm-*co*-DMAAm) triblock copolymer in $CDCl_3$

The efficiency of polymerization was also evaluated by DOSY NMR, one of the powerful tools to characterize block copolymers.[41] DOSY NMR is a two dimensional NMR technique in which the signal decays exponentially due to the self-diffusion behavior of individual molecules. This leads to two dimensions: the first dimension (F_2) accounts for the conventional chemical shift and the second one (F_1) for self-diffusion coefficients (D). Thus, each component in a mixture can be virtually separated, based on its own diffusion coefficient on the diffusion dimension. Fig. 2 shows the DOSY pattern of copolymer T4 in dilute DMSO-d_6. The ^{1}H NMR spectrum exhibits signals corresponding to PLLA (δ=5.1 and 1.5 ppm), NIPAAm (δ=3.9 ppm) and DMAAm (δ=2.7, 2.8, 2.9 and 3.0 ppm). As shown on the DOSY pattern, the ^{1}H NMR signals of PLA and P(NIPAAm-*co*-DMAAm) present the same diffusion coefficient D=2.291×10^{-11} m^2 s^2, in agreement with efficient copolymerization of NIPAAm and DMAAm on the Br-PLLA-Br macroinitiator. No free PNIPAAm was observed since the diffusion coefficient of PNIPAAm in dilute DMSO-d_6 was found to be D=5.248×10^{-11} m^2 s^2.

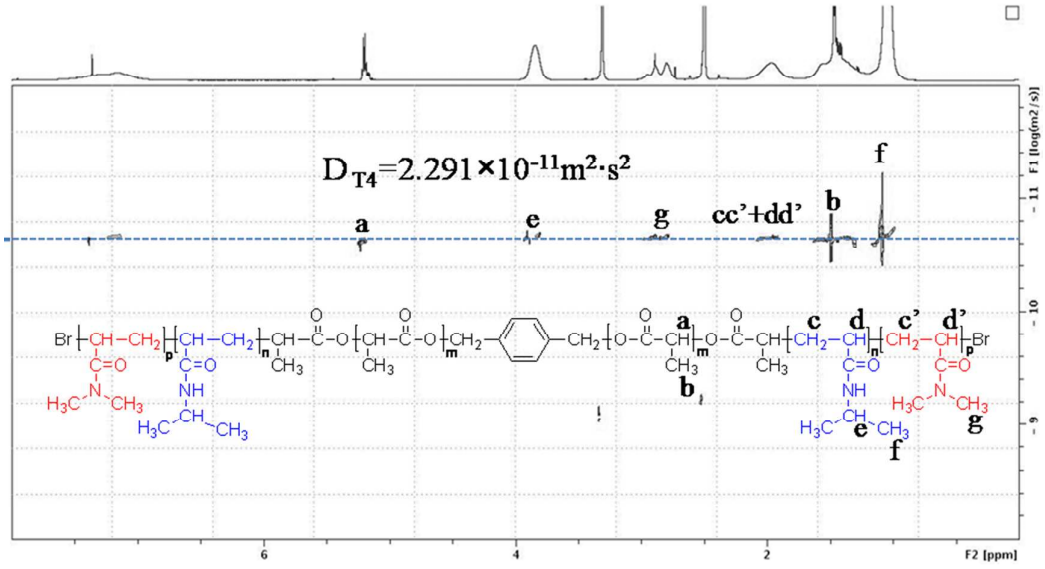

Fig. 2 DOSY NMR spectrum of P(NIPAAm-*co*-DMAAm)-*b*-PLLA-P(NIPAAm-*co*-DMAAm) triblock copolymer in DMSO-d_6.

Fig. 3 shows the GPC traces of the copolymers T1 and T4 in comparison with the Br-PLLA-Br macroinitiator. All the polymers exhibit narrow and monomodal molecular weight distributions. Furthermore, a shift of the copolymer traces towards higher molecular weights is observed as compared to Br-PLLA-Br, indicating successful synthesis of block copolymers.

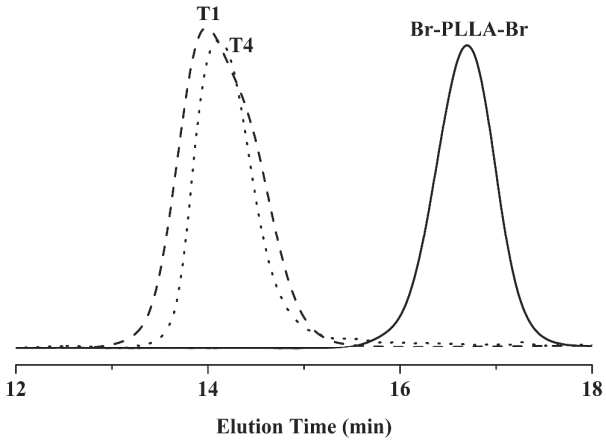

Fig. 3 SEC chromatograms of Br-PLLA-Br macroinitiator and triblock copolymers (T1 and T4)

Table 2 summarizes the characteristics of the various copolymers. The [NIPAAm]/[DMAAm] molar ratio varies from 100/0 to 76/24 in the copolymers. DP_{NIPAAm} varies from 172 to 112, and DP_{DMAAm} varies from 0 to 37. The M_n obtained from SEC ranges from 23600 to 27000 g mol^{-1} with low dispersity ($Đ$=1.10 - 1.18). A good agreement was observed between the $M_{n,NMR}$ and $M_{n,SEC}$ values although the former is slightly lower than the latter.

After polymerization, the catalyst was removed by filtration through a basic alumina column. The copolymers recovered by precipitation in diethyl ether appeared almost colorless. ICP-MS measurements showed that the copper content in the copolymers was between 1 and 3 ppm.

Self-assembling of triblock copolymer micelles in aqueous medium

The physico-chemical properties of the amphiphilic copolymers in aqueous solution were determined in order to evaluate their potential as drug carrier. The different copolymers are water soluble and are able to form micellar aggregates by self-assembly in water using the direct dissolution method. The critical micelle concentration (CMC) was determined by fluorescence spectroscopy using pyrene as hydrophobic probe. Figure 4 shows the I_{337}/I_{333} ratio changes as a function of polymer concentration. The intensity ratio exhibits a substantial increase at a particular concentration, indicating the incorporation of pyrene into micelles. The *CMC* was obtained from the intersection of the two linear regression lines of the plots.

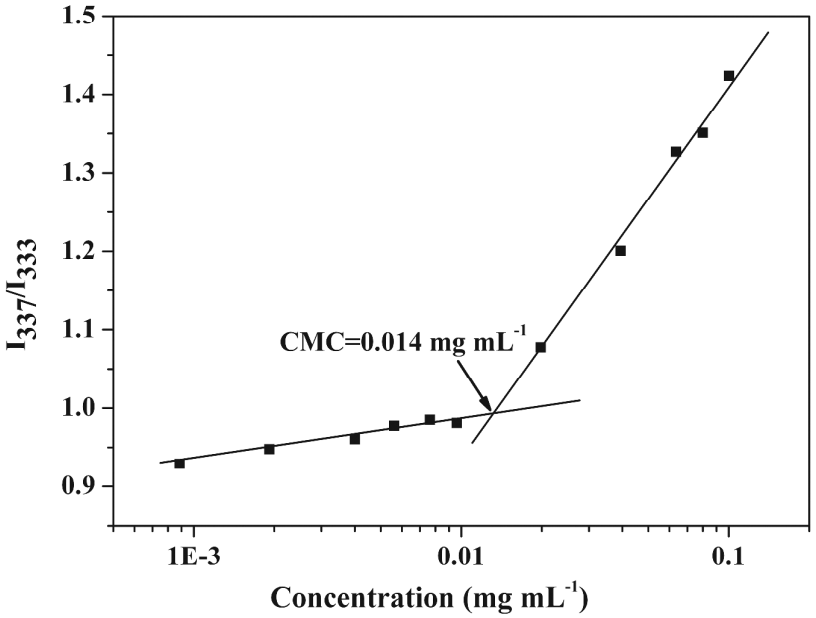

Fig. 4 Plots of the I_{337}/I_{333} ratio changes from pyrene excitation spectra *versus* the concentration of P(NIPAAm-*co*-DMAAm)-*b*-PLLA-*b*-P(NIPAAm-*co*-DMAAm) (T4).

As shown in Table 3, the CMC value ofPNIPAAm-*b*-PLLA-*b*-PNIPAAm (T1) is 0.010 mg mL^{-1}, while those of P(NIPAAm-*co*-DMAAm)-*b*-PLLA-*b*-P(NIPAAm-*co*-DMAAm) are slightly higher. The CMC is dependent on different factors such as the composition, the hydrophilic to hydrophobic ratio, etc. The higher CMC value of P(NIPAAm-*co*-DMAAm)-*b*-PLLA-*b*-P(NIPAAm-*co*-DMAAm) as compared to PNIPAAm-*b*-PLLA-*b*-PNIPAAm is attributed to the presence of more hydrophilic DMAAm units. It is also noted that the CMC values of the copolymers are lower that of the diblock copolymer with NIPAAm/DMAAm/LA ratio of 54/29/14 (0.022 mg mL^{-1}) reported by Akimoto et al.,[34] but higher than those of the copolymers $P(NIPAAm/DMAAm)_{118}$-PLA_{59} and $P(NIPAAm/DMAAm)_{118}$-PCL_{60} reported by Li et al. (0.00184 and 0.00398 mg mL^{-1}, respectively). These findings can be assigned to the fact that higher hydrophobic content leads to lower CMC. The very low CMC values demonstrate the strong tendency of copolymers toward formation of micelles, which is of major importance for the long circulation of micelles in the blood stream after injection induced dilution.[42, 43]

Table 3 Properties of P(NIPAAm-*co*-DMAAm)-*b*-PLLA-*b*-P(NIPAAm-*co*-DMAAm) micelles

Run	$DP_{LA}/DP_{NIPAAm}/DP_{DMAAm}$[a]	[NIPAAm]/[DMAAm][a]	LCST[b] °C	CMC[c] mg mL^{-1}	D_H[d] nm	PDI[d]
T1	40/172/0	100/0	32.3	0.010	40	0.12
T2	40/128/17	88.2/11.8	35.6	-	42	0.17
T3	40/116/25	82.8/17.2	37.1	0.013	42	0.21
T4	40/124/31	80.2/19.8	37.8	0.014	43	0.15
T5	40/112/34	76.9/23.1	38.8	-	55	0.22
T6	40/116/37	76.0:24.0	39.1	0.015	53	0.21

[a] Calculated by NMR. [b] Determined by UV spectroscopy. [c] Determined by fluorescence spectroscopy. [d] Determined by DLS.

Morphology and size distribution of micelles

TEM experiments were performed to examine the morphology of the self-assembling aggregates. As shown in Fig. 5A, the micelles of copolymer T4 are spherical in shape with an average diameter of 32 nm. The size distribution of the copolymer micelles was determined by DLS (Fig. 5B). The micelles exhibit a monomodal and narrow size distribution with an average hydrodynamic diameter of 43 nm and a polydispersity of 0.15. As frequently reported in the literature, the size obtained from DLS is larger than that from TEM. This difference could be attributed to the experimental conditions. In fact, DLS determines the hydrodynamic diameter of micelles in aqueous solution, whereas TEM shows the dehydrated solid state of micelles. Table 3 shows the DLS data of all copolymer micelles in water at 25 ^{o}C. The average diameter varies from 40 to 55 nm with narrow size distribution (*PDI*= 0.15 to 0.22). The size of copolymer micelles increases with increasing the content of hydrophilic DMAAm units. The nano-size of micelles should allow them to escape from the reticuloendothelial system (RES) and preferentially accumulate in tumor tissues through the enhanced permeability and retention (EPR) effect.[44,45] It is noteworthy that the size of copolymer micelles is larger than that of the diblock copolymer (23 nm) reported by Akimoto et al.,[34] but smaller than those of the copolymers P(NIPAAm/DMAAm)$_{118}$-PLA$_{59}$ and P(NIPAAm/DMAAm)$_{118}$-PCL$_{60}$ (170 and 87 nm, respectively) reported by Li et al.[37]

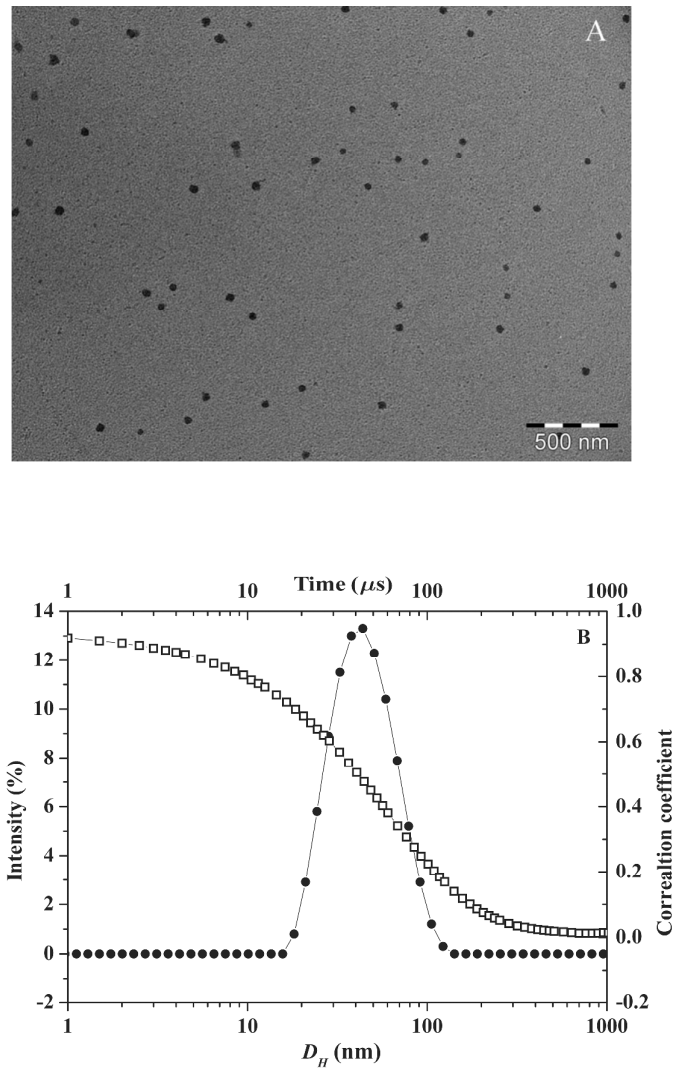

Fig. 5 TEM (A) and DLS (B) results of the self-assembling micelles of copolymer T4 in aqueous medium.

Thermo-responsive behavior of micelles

Our strategy for drug release is to use thermo-sensitive copolymers to target tumor tissue under hyperthermia. Therefore, the LCST should be slightly higher than the body temperature. Thermo-responsive polymers become insoluble when the temperature increases above the LCST due to coil-

to-globule transition. This phase transition can be evidenced by light transmission measurements of micellar solution as a function of temperature.

Fig. 6 shows the transmission changes of different polymeric micelle solutions at 3.0 mg mL^{-1} with increasing temperature. A sharp transmittance decrease is detected around the LCST. The resulting LCST values are listed in Table 3. As expected, the LCST increases from 32.3 to 39.1 ^{o}C with the increase of DMAAm content in the copolymers (Table 3). Moreover, a linear relationship is obtained between the LCST and the molar fraction of DMAAm up to 24 %, as shown in Fig. 6B.

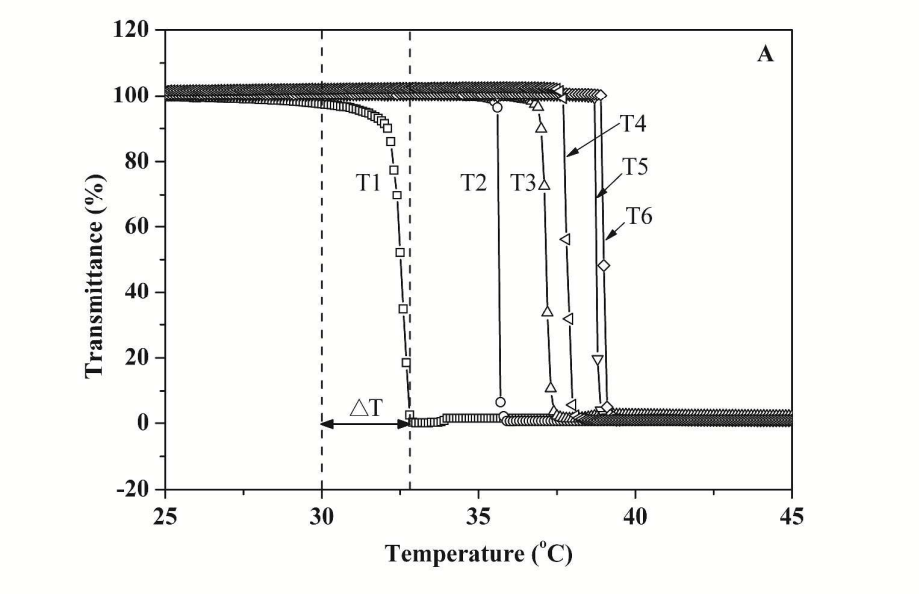

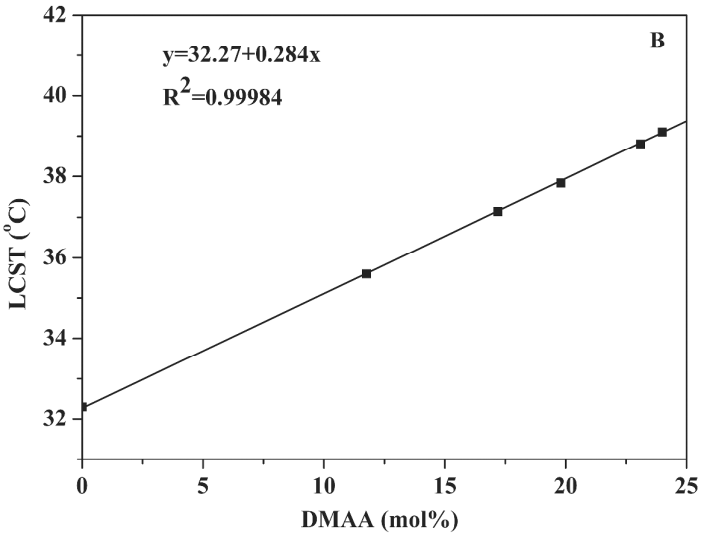

Fig. 6 Plots of transmittance as a function of temperature (A) and plot of LCST values as a function (B) of DMAAm content for copolymer solutions at 3.0 mg mL^{-1}.

Therefore, the LCST can be tuned to temperatures inside tumor tissue by simply increasing the content of DMAAm units in the copolymers. This finding is consistent with literature data. In fact, Shen et al. reported that the LCST linearly increases with increasing the content of DMAAm in P(NIPAAm-*co*-DMAAm) copolymers.[46] The LCST of P(NIPAAm-*co*-DMAAm)-*b*-PLLA diblock copolymers with maleimide endgroup reported by Akimoto et al. [34] and Li et al.[37] is about 40 ^{o}C despite the different P(NIPAAm-*co*-DMAAm) to PLA ratios. In fact, diblock copolymers with maleimide endgroup lead to surface-functional thermo-responsive micelles, and the LCST of micelles can be tuned by mixing hydrophobic DTBz-surface micelles and Mal-surface ones.[34] In our case, the LCST of P(NIPAAm-*co*-DMAAm)-*b*-PLLA-*b*-P(NIPAAm-*co*-DMAAm) triblock copolymers can be precisely adjusted to above the body temperature by varying the NIPAAm to DMAAm ratio, which presents great interest for targeted delivery of anticancer drugs.

Moreover, introduction of DMAAm not only leads to LCST increase of copolymers, but also leads to an extremely narrow phase transition interval within 0.5 ^{o}C. As shown in Fig. 6A, the optical transmittance of PNIPAAm-*b*-PLLA-*b*-PNIPAAm (T1) decreases from 100% to 0 with increasing temperature between 30.0 to 32.8 ^{o}C (ΔT=2.8 ^{o}C). Similar behavior was reported in literature. Indeed, for PNIPAAm-*b*-PLLA diblock copolymer, a broad phase transition of ΔT=5 ^{o}C was observed.[17,18,22] In the case of DMAAm containing copolymer T4, the transmittance decrease from 100 % to 0 occurs in the temperature range of 37.6 to 38.0 ^{o}C, with a phase transition interval ΔT=0.4 ^{o}C. Narrow phase transition intervals below 0.5 ^{o}C were also observed for other DMAAm containing copolymers as shown in Fig. 6A. Nakayama et al. reported phase transition intervals above 3 ^{o}C for P(NIPAAm-*co*-DMAAm)-*b*-PDLLA copolymers obtained by combination of radical polymerization and ROP.[32, 33] On the contrary, Akimoto et al. reported narrow phase transition intervals within 0.5 ^{o}C of such copolymers by combination of RAFT and ROP, which is consistent with our work.[34]

The phase transition of copolymers is illustrated by DLS. Fig. 7 shows the reversible changes of the hydrodynamic diameter distribution depending on temperature. The size of the micelles increases from 35 to 640 nm when the temperature is raised from 25 to 45 ^{o}C. After quickly cooling down to 25 ^{o}C, the micelle size decreases to 38 nm. In fact, P(NIPAAm-*co*-DMAAm) chains are extended and coil-like in water under the LCST. When the temperature approaches the LCST, dehydration of P(NIPAAm-*co*-DMAAm) occurs, leading to precipitation of polymers and aggregation.

The observed phase transition is due to a coil-to-globule transition governed by cooperative dehydration of hydrophilic chains. In the case of PNIPAAm, the hydrogen-bonding site (amido group) is blocked by a bulky hydrophobic group (isopropyl group). The hydrophobic effect is very

important in the LCST behavior of polymer solutions. In fact, a "water cage" is formed around the isopropyl and amide groups in the PNIPAAm blocks. Phase transition occurs upon increasing temperature due to complex dehydration of PNIPAAm at the LCST, excluding water molecules from the water cage.[47-49] The micelles aggregate into large size particles. When randomly distributed DMAAm is introduced, the P(NIPAAm-*co*-DMAAm) chains become more hydrophilic as compared to PNIPAAm, and the LCST transition shifts to higher temperature and becomes sharper. Sharp transition makes the micelles more sensitive to temperature changes and favors quick release of drug above the LCST.

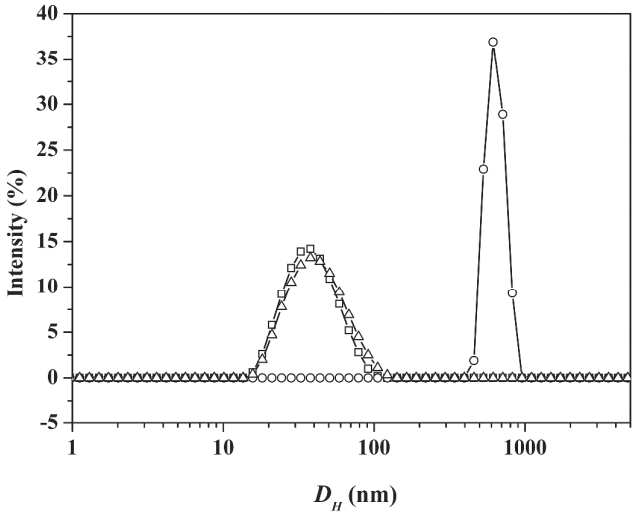

Fig. 7 Reversible changes of the hydrodynamic diameter for T4 micelles at 3 mg mL^{-1} when the temperature is raised from 25 (□) to 45 °C (○), and cooled down to 25 °C (Δ).

In vitro drug release

When used as drug carrier, polymeric micelles are capable of encapsulating hydrophobic drugs. Amphotericin B (AmpB), a poorly water-soluble drug for the treatment of systemic mycosis, was

used as a model drug.[50-52] 2.5 or 5 mg AmpB was loaded in 20 mg polymeric micelles by nano-precipitation. The drug loading content and loading efficiency of AmpB into polymeric micelles are given in Table 4. When the initial drug amount increases from 2.5 to 5 mg, drug content increases from 8.2 to 11.8 %, but the loading efficiency decreases from 83 % to 59 %, which is consistent with literature.[50]

Table 4 Drug loading content and loading efficiency of ampotericin B in polymeric micelles

Sample	Polymer	LCST (°C)	Drug/polymer (mg/mg)	Drug content (%)	Loading efficiency (%)
1	T4	37.8	2.5/20	8.2	83
2	T4	37.8	5/20	11.8	59

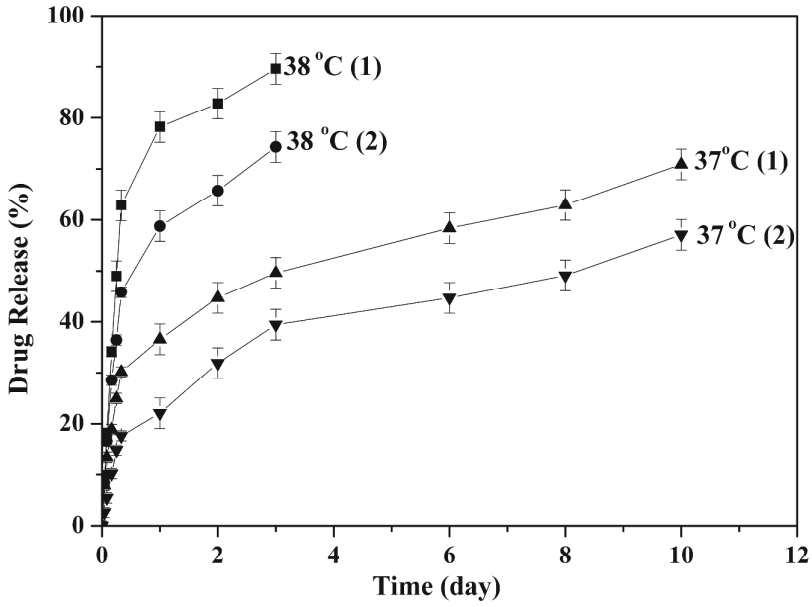

Fig.8 Drug release profiles of AmpB-loaded polymeric micelles (Samples 1 and 2) at 37 and 38 °C in water.

As shown in Fig. 8, an initial burst release of the drug absorbed on the surface of micelles is observed in all cases. Sample 2 with higher drug content exhibits slower release, which could be attributed to the poor solubility of AmpB. On the other hand, the *in vitro* drug release from polymer micelles presents a thermo-sensitive behavior. At temperature below the LCST (37 °C), the release of AmpB is relatively slow. After 3 days, nearly 50 % and 32 % of drug are released for sample 1 and sample 2, respectively. In contrast, at 38 °C which is above the LCST, the release rate is much faster with 90 and 75 % of released drug in both samples. These preliminary results suggest that drug loaded micelles could be injected to a human body and achieve quick drug release at the tumor site where the temperature is higher than the LCST. Thus, the drug release behavior indicates that these copolymers could be potential candidates for applications in targeted delivery of drugs.

Li et al. comparatively studied the release of adriamycin from maleimide end-functional P(NIPAAm-*co*-DMAAm)-*b*-PLA and P(NIPAAm-*co*-DMAAm)-*b*-PCL copolymer micelles under physiological conditions (37 °C and pH = 7.3) and in simulated tumor environment (40 °C and pH = 5.3).[37] The authors observed that only half of entrapped adriamycin was released out within one week under physiological conditions, while about 90 % adriamycin was released within 10 h in simulated tumor environment. Nevertheless, faster degradation of micelles at 40 °C and pH = 5.3 could have contributed to the faster drug release together with the LCST effect. Nakayama et al. studied the release of doxorubicin from P(NIPAAm-*co*-DMAAm)-*b*-PCL and P(NIPAAm-*co*-DMAAm)-*b*-P(LA-*co*-CL) copolymer micelles below and above the LCST.[32] No difference was detected in the case of P(NIPAAm-*co*-DMAAm)-*b*-PCL at 42.5 °C and 37 °C. In contrast, the release of doxorubicin is much faster at 41 °C than that at 35 °C in the case of P(NIPAAm-*co*-DMAAm)-*b*-

P(LA-*co*-CL). Again, degradation of micelles plays a key role in drug release because P(LA-*co*-CL) degrades much faster than PCL.[53] In our case, the faster release of AmpB can be assigned to the destabilization of micelles above the LCST since little difference of degradation is detected at 38 °C and 37 °C.

Cytocompatibility

In vitro cytotoxicity is generally evaluated by MTT assay for the screening of biomaterials.[54] MTT assay is based on the reaction between MTT and mitochondrial succinate dehydrogenases in living cells to form a purple formazan which is soluble in DMSO but insoluble in water. The OD value of formazan-DMSO solution is considered to be proportional to the number of living cells.

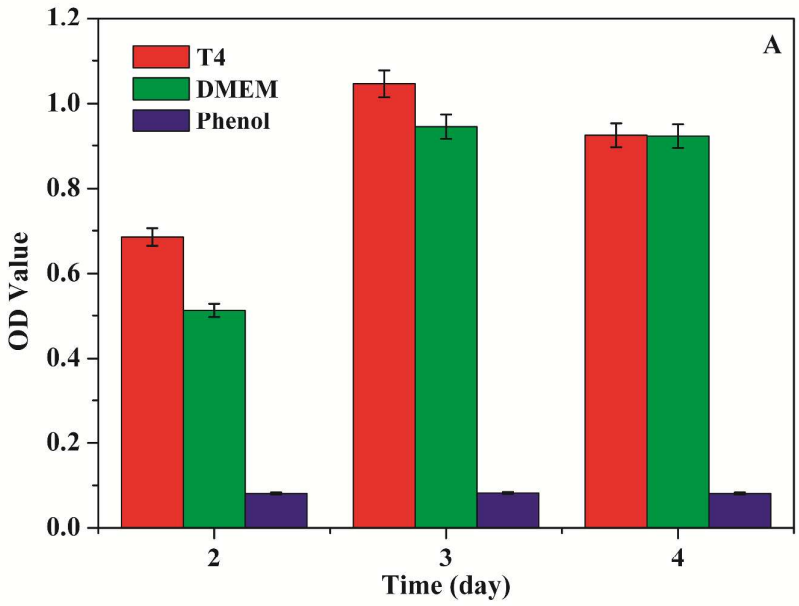

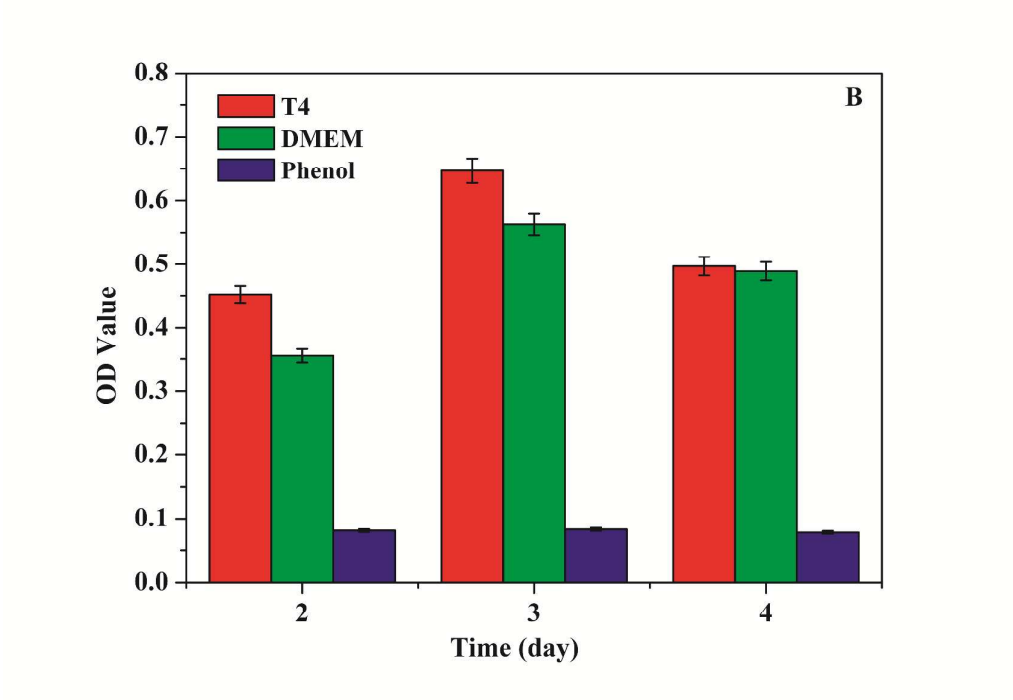

Fig. 9 Optical density values of MCM (A) and MEF (B) solutions after 2, 3 and 4 days culture in DMEM with copolymer substrate (T4), and controls (DMEM and 5% phenol)

The effect of copolymer T4 on the growth of MCM and MEF cells is shown in Figure 9, in comparison with controls (DMEM medium and 5 % phenol). The OD values on polymer substrate are slightly higher than those in the culture solution, and much higher than those in phenol. The RGR values of copolymer T4 are well above 100% during 4 days incubation with MCF and MEF cells, corresponding to a cytotoxicity level of 0 (Table 5).

Table 5 RGR values of copolymers T4 with MCM and MEF cells during 4 days incubation

Cell	RGR (%)		
	2 days	3 days	4 days
MCM	133.8±1.1	110.8±3.0	100.2±1.2
MEF	127.3±1.6	114.9±2.0	101.6±1.0

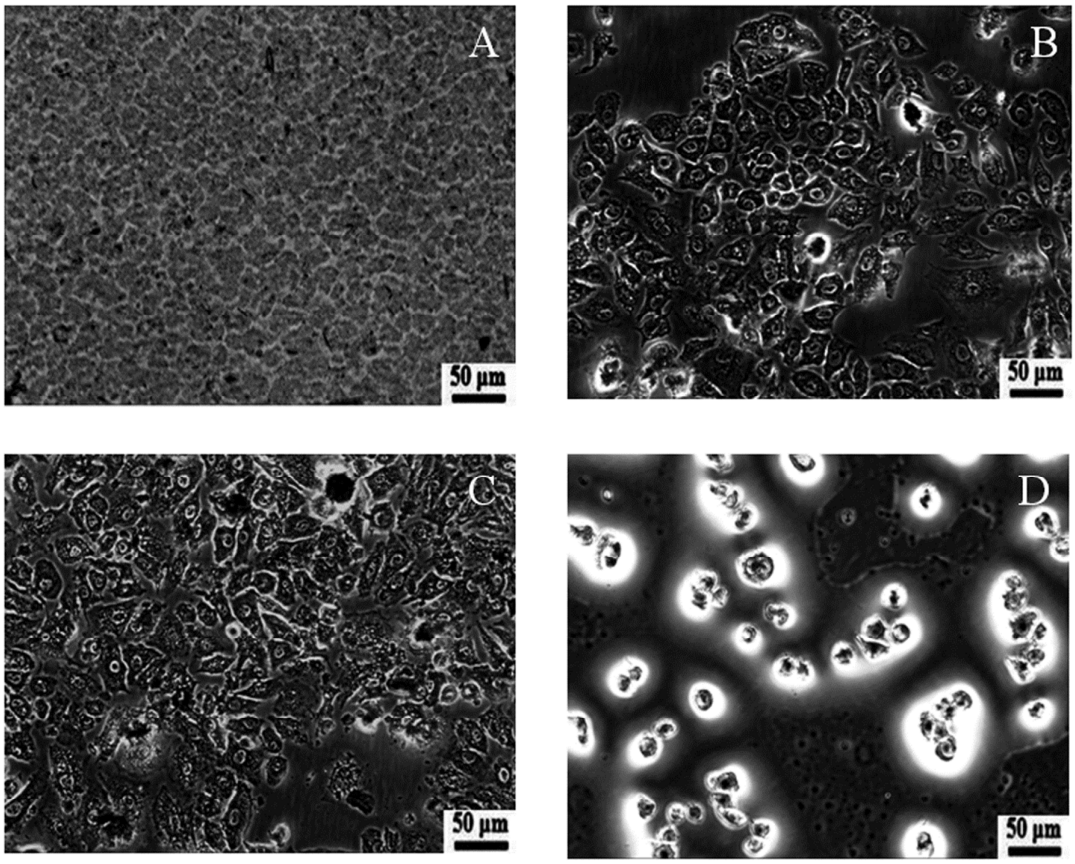

Fig. 10 Microscopic images of cells stained by NR after 3 days culture in different media: (A) Copolymer T4 substrate without cell; (B) MCM cells on polymer substrate in DMEM; (C) MEF cells on polymer substrate in DMEM; (D) MEF cells in 5 % phenol medium

Figure 10 shows the morphology of cells after 3 days culture. Large number of cells died in the toxic phenol medium (Fig. 10D). On the contrary, cell adhesion and proliferation are observed on the copolymer substrate (Fig. 10B and Fig. 10C). Cells exhibit spindle, polygon or oval shapes, and the pseudopodium of cells stretches out. Therefore, MTT assay and cell morphology observation indicate that P(NIPAAm-*co*-DMAAm)-*b*-PLLA-*b*-P(NIPAAm-*co*-DMAAm) copolymers presents outstanding cytocompatibility and could be used for biomedical applications.

Conclusion

P(NIPAAm-*co*-DMAAm)-*b*-PLLA-*b*-P(NIPAAm-*co*-DMAAm) triblock copolymers were prepared by ATRP using Br-PLLA-Br as macroinitiator. The resulting copolymers present well defined molecular weights and narrow dispersities. The LCST of the copolymers linearly increases from 32.3 to 39.1 °C with increasing the DMAAm content. Self-assembling micelles were prepared by dissolving the copolymers in aqueous medium. The copolymers have very low CMC (10 to 15 μg mL^{-1}) and nano-size (40 to 55 nm). The presence of DMAAm units in the copolymers leads to an extremely sharp phase transition, as compared to PNIPAAm-*b*-PLLA-*b*-PNIPAAm copolymers. Moreover, reversible size changes were observed when the micelle solutions was heated from 25 to 45 ^{o}C and then cooled down to 25 ^{o}C. Much faster drug release is detected at temperatures above the LCST in *in vitro* studies. The MTT assay and cell morphology observation confirm the good biocompatibility of these thermosensitive copolymers.

Therefore, the small size and low CMC, the LCST slightly above the body temperature, the rapid phase transition at LCST, the thermo-responsive drug release behavior above LCST, and the good cytocompatilibity indicate that P(NIPAAm-*co*-DMAAm)-*b*-PLLA-*b*-P(NIPAAm-*co*-DMAAm) copolymers are promising candidates for applications in targeted delivery of anticancer drugs.

References

1 A. K. Bajpai, S. K. Shukla, S. Bhanu and S. Kankane, *Prog. Polym. Sci.,* 2008, **33**, 1088-1118.

2 A. Kumar, A. Srivastava, I. Y. Galaev and B. Mattiasson, *Prog.Polym. Sci.*, 2007, **32**, 1205-1237.

3 B. Guillerm; V. Darcos, V. Lapinte, S.Monge, J.Coudane, J.J. Robin, *Chem. Comm*., 2012, **48**, 2879-2881.

4 W.Y. Ooi, M. Fujita, P.J. Pan, H.Y. Tang, K. Sudesh, K. Ito, N. Kanayama, T. Takarada and M. Maeda, *J. Colloid Interface Sci.*, 2012, **374**, 315-320.

5 A. Wang, C. Tao, Y. Cui, L. Duan, Y. Yang and J. Li, *J. Colloid Interface Sci.*, 2009, **332**, 271-279.

6 C. H. Hu, X. Z. Zhang, L. Zhang, X. D. Xu and R. X. Zhuo, *J. Mater. Chem.*, 2009, **19**, 8982-8989.

7 Y. Liu, X. Cao, M. Luo, Z. Le and W. Xu, *J. Colloid Interface Sci.*, 2009, **329**, 244-252.

8 P. VanRijn, H. Park, K. O. Nazli, N. C. Mougin and A. Boker, *Langmuir*., 2009, **29**, 276-284.

9 N.M. Matsumoto, P. Prabhakaran, L.H. Rome and H.D. Maynard, *ACS Nano*., 2013, **7**, 867-878.

10 H. Wei, S. X. Cheng, X. Z. Zhang and R.X. Zhuo, *Prog. Polym. Sci*., 2009, **34**, 893-910.

11 H. G. Schild, *Prog. Polym. Sci*., 1999, **17**,163-249.

12 H. Senff and W. Richtering, *Collioid Polym. Sci*., 2000, **278**, 830-840.

13 A. C. Albertsson and I. Varma, *Adv. Polym. Sci*., 2002, **157**, 1-40.

14 G. S. He, L. L. Ma, J. Pan and S. Venkatraman, *Int. J. Pharm*., 2007, **334**, 48-55.

15 L. Yang, A. E. Ghzaoui and S. M. Li, *Int. J. Pharm*., 2010, **400**, 96-103.

16 I. Barwal, A. Sood, M. Sharma, B. Singh and S.C. Yadav, *Colloids Surf. B: Biointerfaces*, 2007, **101**, 510-516.

17 F. Kohori, K. Sakai, T. Aoyagi, M. Yokoyama, Y. Sakuraib and T. Okano, *J. Controlled Release*, 1998, **55**, 87-98.

18 J. Qin, Y. S. Jo, J. E. Ihm, D. K. Kim and M. Muhammed, *Langmuir*, 2005, **21**, 9346-9351.

19 E. Ayano, M. Karaki, T. Ishihara, H. Kanazawa and T. Okano, *Colloids Surf. B: Biointerfaces*, 2012, **99**, 67-73.

20 Y.Z. You, C.Y. Hong, W.P. Wang, W.Q. Lu and C.Y. Pan, *Macromolecules*., 2004, **37**,9761-9767.

21 M. Hales, C.T. P. Barner-kowollik, M. Davis and H. Stenzel, *Langmuir*, 2004, **20**, 10809-10817.

22 H. Wei, X.Z. Zhang, C. Cheng, S. X. Cheng and R.X. Zhuo, *Biomaterials*, 2007, **28**, 99-107.

23 S.J.T. Rezaei, M.R. Nabid, H. Niknejad and A. A. Entezami, *Int. J. Pharm.*, 2012, **437**, 70-79.

24 S.J.T. Rezaei, M.R. Nabid, H. Niknejad and A. A. Entezami. *Polymer*, 2012, **53**, 3485-3497.

25 F. N. Chearuil and O. I. Corrigan, *Int. J. Pharm*., 2009, **366**, 21-30.

26 J. Zhang and R. D. K. Misra, *Acta Biomaterialia*, 2007, **3**,838-850.

27 F. Kohori, K. Sakai, T. Aoyagi, M. Yokoyama, M. Yamato, Y. Sakurai and T. Okano, *Colloids Surf., B: Biointerfaces*, 1999, **16**, 195-205.

28 S.Q. Liu, Y.Y. Yang, X.M. Liu and Y.W. Tong, *Biomacromolecules*, 2003, **4**, 1784-1793.

29 S. Q. Liu, Y. W. Tong and Y.Y. Yang, *Biomaterials*, 2005, **26**,5064-5074.

30 S. Q. Liu, Y. W. Tong and Y. Y. Yang, *Mol. Biosyst.*, 2005, **1**, 158-165.

31 S.Q. Liu, N. Wiradharma, S.J. Gao, Y. W. Tong and Y.Y. Yang, *Biomaterials*, 2007, **28**, 1423-1433.

32 M. Nakayama, T. Okano, T. Miyazaki, F. Kohori, K. Sakai and M. Yokoyama, *J. Controlled Release*, 2006, **15**, 46-56.

33 M. Nakayama, J. E. Chung, T. Miyazaki, M. Yokoyama, K. Sakai and T. Okano, *React. Func. Polym.*, 2007, **67**, 1398-1407.

34 J. Akimoto, M. Nakayama, K. Sakai and T. Okano, *J. Polym. Sci. Part A. Polym. Chem*., 2008, **46**, 7127-7137.

35 J. Akimoto, M. Nakayama, K. Sakai and T. Okano, *Biomacromolecules*, 2009, **10**, 1331-1336.

36 J. Akimoto, M. Nakayama, K. Sakai and T. Okano, *Mol. Pharm.*, 2010, **7**, 926-935.

37 W. Li, J. F. Li, J. Gao, B. H. Li, Y. Xia, Y. C. Meng, Y. S. Yu, H. W. Chen, J. X. Dai, H. Wang and Y. J. Guo, *Biomaterials.*, 2011, **32**, 3832-3844.

38 Y. F. Hu, V. Darcos, S. Monge and S. M. Li, *J. Polym. Sci. Part A. Polym. Chem*., 2013, **51**, 3274-3283.

39 G. Masci, L. Giacomelli and V. Crescenzi, *Macromol. Rapid. Commun*., 2004, **25**, 559-564.

40 K. Bauri, S. Roy, S. Arora, R. Dey, A. Goswami, G. Madras and P. De, *J. Therm Anal Calorim*, 2013, 111, 753-761.

41 Y. Bakkour, V. Darcos, S.M. Li and J. Coudane, *Polym. Chem.,* 2012, **3**, 2006-2010.

42 M. Yokoyama, T. Okano, Y. Sakurai, H. Ekimoto, C. Shibazaki and K. Kataoka, *Cancer Res.*, 1991, 51, 3229-3236.

43 M. L. Adams, A. Lavasanifar and G. S. Kwon, *J. Pharm. Sci.*, 2003, **92**, 1343-1355.

44 Y. Yan, G.K. Such, A.P.R. Johnston, J.P. Best and F. Caruso, *ACS Nano*., 2012, **6**, 3663-3669.

45 C. Oerlemans, W. Bult, M. Bos, G. Storm, J.F. Nijsen and W. Hennink, *Pharm. Res.,* 2010, **27**, 2569-2589.

46 Z. Shen, K. Terao, Y. Maki, T. Dobashi, G. Ma and T. Yamamoto. *Colloid Polym. Sci*.2006, **284**, 1001-1007.

47 E. C. Cho, J. Lee and K. Cho, *Macromolecules*., 2003, **36**, 9929-9934.

48 Y. Okada and F. Tanaka, *Macromolecules*., 2005, **38**, 4465-4467.

49 Y. Ono and T. Shikata, *J. Am. Chem. Soc*., 2006, **128**, 10030-10031.

50 K.C. Choi, J.Y. Bang, P.I. Kim, C. Kim and C.E. Song, *Int. J. Pharm.*, 2008, **335**, 224-230.

51 T. A. Diezi, J. K. Takemoto, N. M. Davies and G. S. Kwon, *J. Pharm. Sci.*, 2011, **100**, 2064-2070.

52 M. L. Adams, D. R. Andes and G. S. Kwon, *Biomacromolecules*, 2003, **4**, 750-757.

53 S. M. Li, J. L. Espartero, P. Foch, M. Vert, *J Biomater.Sci.,Polym. Ed*, 1996, **8**, 165-187.

54 Y. L. Luo, C. H. Zhao, F. Xu, Y. S. Chen. *Polym. Adv.Technol,* 2012, 23, 551-557.